Structural Engineering and Mechanics, *Vol. 51, No. 2 (2014) 277-297*
DOI: http://dx.doi.org/10.12989/sem.2014.51.2.277

The effect of impact with adjacent structure on seismic behavior of base-isolated buildings with DCFP bearings

Morteza Bagheri* and Faramarz Khoshnoudian[a]

Department of Civil Engineering, Amirkabir University of Technology, Hafez St., Tehran, Iran

(Received October 9, 2013, Revised May 1, 2014, Accepted May 9, 2014)

Abstract. Since the isolation bearings undergo large displacements in base-isolated structures, impact with adjacent structures is inevitable. Therefore, in this investigation, the effect of impact on seismic response of isolated structures mounted on double concave friction pendulum (DCFP) bearings subjected to near field ground motions is considered. A non-linear viscoelastic model of collision is used to simulate structural pounding more accurately. 2-, 4- and 8-story base-isolated buildings adjacent to fixed-base structures are modeled and the coupled differential equations of motion related to these isolated systems are solved in the MATLAB environment using the SIMULINK toolbox. The variation of seismic responses such as base shear, displacement in the isolation system and superstructure (top floor) is computed to study the impact condition. Also, the effects of variation of system parameters: isolation period, superstructure period, size of seismic gap between two structures, radius of curvature of the sliding surface and friction coefficient of isolator are contemplated in this study. It is concluded that the normalized base shear, bearing and top floor displacement increase due to impact with adjacent structure. When the distance between two structures decreases, the base shear and displacement increase comparing to no impact condition. Besides, the increase in friction coefficient difference also causes the normalized base shear and displacement in isolation system and superstructure increase in comparison with bi-linear hysteretic behavior of base isolation system. Totally, the comparison of results indicates that the changes in values of friction coefficient have more significant effects on 2-story building than 4- and 8-story buildings.

Keywords: double concave friction pendulum; isolation period; radius of curvature; friction coefficient; impact; near-field ground motions

1. Introduction

Seismic isolation technology is a new method of anti-seismic design of structures, which has been more widely used in the recent years. This approach based on seismic design criteria has emerged aiming at reducing the seismic damage by providing an isolation system at the base of a structure. Kelly (1986), Su *et al*. (1989) and Skinner *et al*. (1993) provided comprehensive reviews on isolation devices and techniques. The simplest sliding system device is a pure-friction (P-F) system without any restoring force (Mostaghel and Tanbakuchi

*Corresponding author, Former Master Student, E-mail: Bagheri_civil@aut.ac.ir
[a]Associate Professor, E-mail: Khoshnud@aut.ac.ir

http://www.techno-press.org/?journal=sem&subpage=8 ISSN: 1225-4568 (Print), 1598-6217 (Online)

1983, Yang *et al*. 1990, Khoshnoudian and Haghdoust 2009). In addition, some researchers have studied the sliding systems with restoring force such as the resilient-friction base isolator (R-FBI) system (Mostaghel and Khodaverdian 1987), the friction pendulum system (FPS) (Zayas *et al*. 1990) and variable friction pendulum system (VFPS) (Murnal and Sinha 2002, Panchal and Jangid 2008).

Double concave friction pendulum (DCFP) system is a newly developed device which is similar to FPS system with two sliding surfaces. The behavior of a FPS can be made more effective by introducing a second sliding surface. DCFP system has been used in a few buildings in Japan (Hyakuda *et al*. 2001) and a bridge in Canada (Constantinou 2004). In contrary to the buildings in Japan, the bearings sliders used in Teslin Bridge were all articulated, as proposed by Tsai *et al*. (2003). Theoretical modeling of DCFPs has been studied by Constantinou (2004), Tsai *et al*. (2004, 2005) and Fenz and Constantinou (2006). Kim and Yun (2007) studied the advantages of tri-linear DCFP over the bi-linear DCFP for isolating of the bridges from strong motions. They concluded that tri-linear DCFP causes reduction effect on the base shear of the pier in the range of 15%-40% over bi-linear DCFP system. Their investigation was performed only for bridges and there is no special study on the structures isolated with bi-linear and tri-linear DCFP bearings. Most of the previous investigations regarded structures isolated with DCFP subjected to one or two horizontal components of earthquakes. The effect of vertical component of earthquake on the responses of the isolated structure using DCFP systems was studied using some essential parameters. It was demonstrated that neglecting the vertical component of earthquake causes the maximum error of 5 and 22 percent (in the same order) in determining the peak bearing displacement and base shear of the structure respectively (Khoshnoudian and Rabie 2010).

With the addition of flexible layer at foundation level the peak base displacements increase during earthquakes and the isolated structure can collide upon adjacent structures like boundary retaining walls, entrance ramps, etc. Such incidence of impact in case of base-isolated buildings has been reported during 1994 Northridge earthquake (Nagarajaiah and Sun 2001).

Compared to the extensive research works on poundings of conventional buildings and bridges, limited research studies have been carried out for poundings of seismically isolated buildings. The first attempt to study impact problem in case of a base-isolated structure was made by Tsai (1997) and Malhotra (1997). Tsai (1997) observed the amplification of acceleration response during pounding with the surrounding moat wall at the isolation level. Malhotra (1997) concluded that the base shear force increases with the stiffness of the superstructure or training wall, while sometimes it becomes higher than the total weight of the seismically isolated building.

Matsagar and jangid (2003) also numerically examined the pounding of seismically isolated multi-degree-of-freedom (MDOF) structures, for various types of seismic isolation systems. They concluded that poundings affect the response of a seismically isolated building more when the latter has a flexible superstructure, an increased number of stories or relatively stiff adjacent structures. The study of poundings of a seismically isolated building with the surrounding moat wall revealed the detrimental effects of structural impacts on the effectiveness of seismic isolation (Komodromos *et al*. 2007, Komodromos 2008). In those research works, the behavior of the seismic isolation system was assumed to be linear elastic, while no other adjacent buildings were considered in the simulations. Recently, Agarwal *et al*. (2007) have examined the case of poundings between two-story buildings that were taken to be either fixed-supported or seismically isolated. In the case of seismically isolated buildings, a sliding isolation system with varying friction was considered. Furthermore, the case of poundings between a seismically isolated building and a fixed-supported building was not taken into account and the simulation involved

only buildings with two degrees of freedom. Panayiotis and Komodromos (2010) investigated, through numerical simulations, the effects of potential pounding incidences on the seismic response of a typical four story isolated building. Their simulations have revealed that even if a sufficient gap with the surrounding moat wall cannot ensure that the building will not eventually collide with neighboring buildings due to the deformations of their superstructures.

The past research in the area of base isolation considering impact with adjacent structure has focused on the use of a linear impact spring employed in commercial software easily. However, energy loss during impact cannot be modeled. Therefore, the linear elastic model is not capable of simulating in a satisfactory way the behavior of the real isolation system. But, contact elements which account energy dissipation represent a better estimation of behavior in base isolated buildings during impact. The linear viscoelastic model of collisions (Kelvin model) has been initially proposed by Anagnostopoulos (1988). In the case of structural poundings, Muthukumarand DesRoches (2006) used a modified Hertz model with nonlinear damping to take energy dissipation into account and estimate the contact forces to investigate structural impact.

Despite the previous research on earthquake-induced poundings of seismically isolated buildings, there is still a necessity for further investigation of the problem, using more effective modeling approaches and more new base isolation systems. Therefore, the present study is carried out using non-linear viscoelastic impact element (Jankowski 2005) on modeling of collision in isolated buildings supported on DCFP bearings. The nonlinear viscoelastic impact model was proposed by Jankowski (2005), which can reasonably account for the physical nature of pounding is implemented in the present study. The superstructure is idealized as shear type building and fixed-supported multi-story buildings are considered to be located next to a seismically isolated structure. Therefore, impact may occur with the adjacent buildings either at the base of the seismically isolated building or at the levels of the floors of their superstructures. The isolated system is subjected to single horizontal component of near-field earthquake ground motion. Furthermore, the effects of certain parameters, such as separation gap distance, isolation period, superstructure period, radius of curvature of the sliding surface and friction coefficient of isolator is investigated.

2. Presentation of implemented model

2.2 Modeling of double concave friction pendulum (DCFP)

The behavior of the isolated structural system is simulated using a bilinear inelastic model, since it represents satisfactorily the behavior of the most commonly used seismic isolation systems such as the Friction Pendulum Systems (FPS).

The shear force-horizontal deformation relationship of the FPS bearing under unidirectional displacement can be described assuming the Coulomb friction as (Constantinou 2004, Fenz and Constantinou 2006)

$$F = \frac{N}{R}u + \mu N sign(\dot{u}) \tag{1}$$

Where F is the horizontal restoring force developed in the isolation bearing; N represents the weight of the structure acting on the isolator (superstructure); R is the radius of curvature of the spherical surface and μ is the sliding coefficient of friction of the bearing interface.

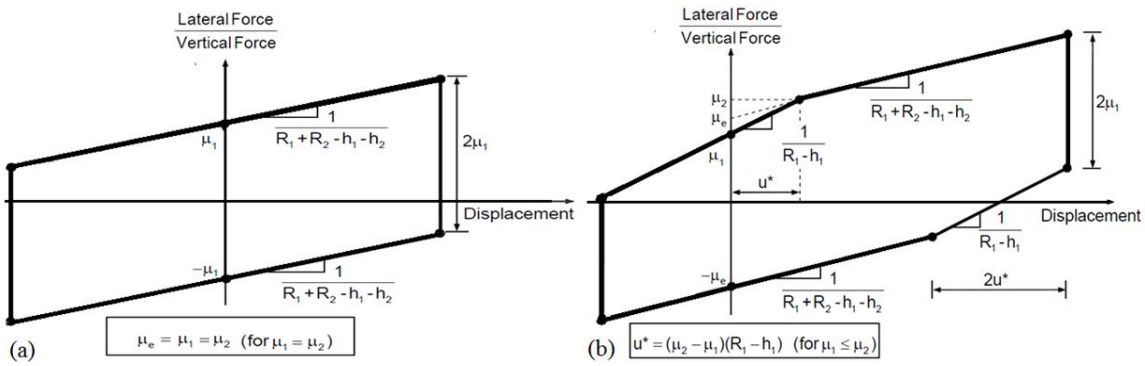

Fig. 1 The hysteretic curve of: (a) bi-linear DCFP (b) tri-linear DCFP (Fenz and Constantinous 2006)

Mathematically, this friction coefficient is known to be velocity dependent and can be expressed as (Mokha *et al*. 1991, Tsopelas *et al*. 1996, Constantinou 2004, Fenz and Constantinou 2006)

$$\mu = f_{\max} - (f_{\max} - f_{\min})e^{-a|\dot{u}|}\dot{u}_i \tag{2}$$

Here, $f_{\max}$ is the maximum sliding friction coefficient at high sliding velocity; $f_{\min}$ is the minimum sliding friction coefficient at essentially zero sliding velocity; a is a constant for given bearing pressure and condition of interface. This parameter controls the variation of friction coefficient with sliding velocity.

When sliding surfaces with equal friction coefficient are used (μ_2=μ_1), there is simultaneous sliding on both surfaces over the entire range of motion, regardless of radii of curvature. The hysteretic behavior is so called bi-linear like that of the traditional FPS (Constantaniou 2004). During this condition, the isolation period (T_i) can be described by Eq. (3) (Kim and Yun 2007). Fig. 1 illustrates the hysteretic curves of bi-linear DCFP and tri-linear DCFP.

$$T_i = 2\pi\sqrt{\frac{R_1 + R_2}{g}} = \sqrt{T_1^2 + T_2^2} \tag{3}$$

$$T_1 = 2\pi\sqrt{\frac{R_1}{g}} \tag{4}$$

$$T_2 = 2\pi\sqrt{\frac{R_2}{g}} \tag{5}$$

T_1 and T_2 are restoring periods of the lower and upper sliding surfaces respectively.
R_1 and R_2 are radius of curvature of the lower and upper sliding surfaces in the same order.

When friction coefficient is different on the upper and lower concave sliding surfaces ($\mu_2 \neq \mu_1$), motion initiates on the surface of least friction coefficient and continues on this surface for a distance u^*. During this sliding regime, the isolation period equals T_1 for $\mu_1 < \mu_2$ and equals T_2 for $\mu_1 > \mu_2$. After the displacement exceeds u^*, there is sufficient horizontal force to initiate sliding on

the surface of higher friction and motion continues with simultaneous sliding on both sliding surfaces. For tri-linear DCFPs, an equivalent friction coefficient and u^* are assumed by following equations (Constantaniou 2004)

$$\mu_{eq} = \frac{\mu_1(R_1 - h_1) + \mu_2(R_2 - h_2)}{R_1 + R_2 - h_1 - h_2} \tag{6}$$

$$u^* = (\mu_2 - \mu_1)(R_1 - h_1) \tag{7}$$

h_1: Distance between center of the lower sliding surface and center of the articulated mass.
h_2: Distance between center of the upper sliding surface and center of the articulated mass.

2.2 Impact model

According to several uncertainties in mathematical modeling of pounding, the researchers usually have modeled contact using either a stereomechanical approach or a contact element approach. The first one uses energy and momentum conservation principles and does not consider transient stresses and deformations and the duration of impact in the colliding bodies (Goldsmith 1960, Ruangrassamee and Kawashima 2001, DesRoches and Muthukumar 2002). The second approach for modeling of pounding is to simulate the pounding force during impact (Jankowski 2005). The description of the various impact models according to contact element approach are presented below.

2.2.1 Linear contact elements

(a) Linear elastic model

Owing to its simplicity, these elements have been widely used as the simplest contact element to model impact. However, the elastic contact elements cannot account the energy dissipation during impact (Maison and Kasai 1992, Filiatrault *et al*. 1995, Zanardo *et al*. 2002, Kim and Shinozuka 2003).

(b)Linear viscoelastic model (Kelvin-Voigt model)

When the structures come into contact, the energy is dissipated and the damper accounts for energy loss during the whole time of impact. The Kelvin-Voigt element utilizes a linear spring in parallel with a damper has been initially used by Anagnostopoulos (1988) to study impact between adjacent buildings. The disadvantage of the linear spring-damper element is that its viscous component is active with the same damping coefficient during the whole time of collision that is not consistent with the reality (Goldsmith 1960). Moreover, this model exhibits an initial jump of the impact force values on impact because of the damping term (Ye and Li 2009).

2.2.2 Non-linear contact elements

(a)Hertz model with non-linear damper (Hertz damp model)

Hertz model that uses a varying damping and a nonlinear impact spring (Hertz damp model) has been introduced first by Muthukumarand DesRoches (2006) for the simulation purposes of structural pounding. Hertz damp model does not suffer from the disadvantage of the Hertz model and accounts for the energy dissipation during impact.

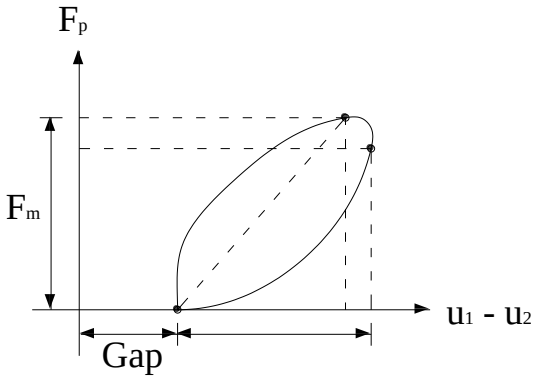

Fig. 2 Non-linear viscoelastic contact element (Jankowski 2005)

(b)Nonlinear viscoelastic model

To overcome the disadvantages of the linear viscoelastic and the non-linear elastic models Jankowski proposed the nonlinear viscoelastic model based on Hertz's contact law (Jankowski 2005). In the model proposed, he substituted the stiffness constant used in damping equation with $k_p\delta(t)$ (see Eq. (8)) correlated with linear viscoelastic model. Additionally, a non-linear damper is comprised to the non-linear impact spring during the approach period of the collision, while during the restitution phase, the energy dissipation is omitted (Jankowski 2005). However, the impact force-time curve obtained from this impact model is not smoothly varied between the approach phase and restitution period of the collision (Ye and Li 2009). Furthermore, on the contrary with other impact models, the impact force reaches to its maximum value a little before the end of compression phase. The past researches showed that the nonlinear viscoelastic impact model is more accurate than the other contact elements and simulates the collision more realistically (Jankowski 2005, 2006). Therefore, this model has been employed in this investigation.

Herein, the governing equations for this model can be expressed as:

$$F_p(t)=\begin{cases} k_p\delta(t)^{\frac{3}{2}}+c_p(t)\delta(t) & \delta(t)>0 \quad \dot{\delta}(t)>0 \\ k_p\delta(t)^{\frac{3}{2}} & \delta(t)>0 \quad \dot{\delta}(t)\le 0 \\ 0 & \delta(t)\le 0 \end{cases} \tag{8}$$

$$c_p(t)=2\xi_p\sqrt{k_p\frac{m_1m_2}{m_1+m_2}}\delta(t)^{\frac{1}{4}} \tag{9}$$

According to the Jankowski's research (Jankowski 2005) for study the impact of a spherical concrete pendulum striker, the following values of parameters defining viscoelastic pounding force model is used in this study

$$k_p=2.75\times10^6\,\frac{KN}{m^{3/2}} \quad \xi_p=0.35(e=0.65)$$

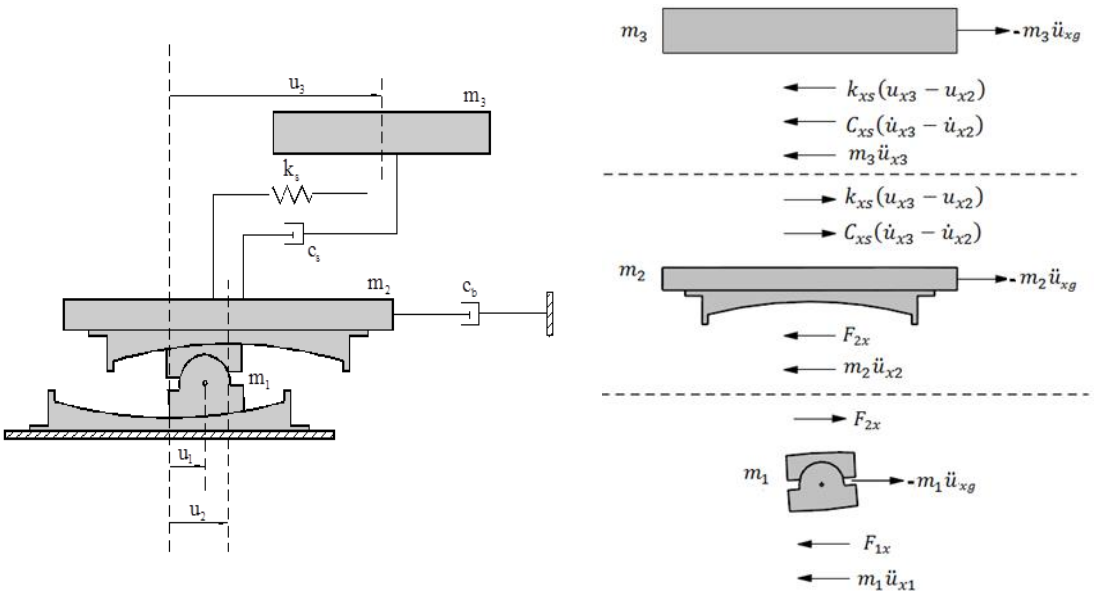

Fig. 3 (a) Schematic model of a one-story base-isolated structure; (b) Free body diagram (Fenz 2008)

2.3 Dynamic modeling of the building and isolation system

In this section the superstructure has been modeled as a SDOF system schematically. In order to formulate the equation of motion of a base-isolated structure mounted on a DCFP isolator, a schematic model of a SDOF system is shown in Fig. 3(a). In this Figure; m_1 is a very small mass that must be assigned to represent the articulated slider, m_2 is the mass of basement and m_3 is the mass of superstructure. k_s and c_s represent the stiffness and equivalent viscous damping coefficient of the superstructure respectively. Also, c_b is indicative of the damping coefficient of any dampers.

The restoring force mechanism related to the curvature of the sliding surface can be described as

$$F_i = \frac{W}{R_{effi}} u_i + \mu_i W Z_i + k_{ri}(|u_i| - d_i) sign(u_i) H < |u_i| - d_i > \tag{10}$$

Where u is the relative displacement of slider to the concave surface; W is the weight of the superstructure; R_{effi} is the effective radius of curvature of the sliding surface; μ_i is the coefficient of friction between the slider and sliding surface dependent to velocity (see Eq. (2)) and Z_i is the non-dimensional hysteretic displacement component equals to -1 or 1. k_{ri} is the stiffness related to maximum displacement; d_i is the displacement capacity of surface i and H is a Heaviside function.

According to the free body diagram (Fig. 3(b)) relevant to this model, the force equilibrium conditions at three masses may yield the following equations of motion

$$m_3\ddot{u}_3 + c_S(\dot{u}_3 - \dot{u}_2) - k_S(u_3 - u_2) = -m_3\ddot{u}_g(t) \tag{11}$$

$$m_2\ddot{u}_2+\frac{W}{R_{eff\,2}}(u_2-u_1)-c_S(\dot{u}_3-\dot{u}_2)-k_S(u_3-u_2)-c_b\dot{u}_2+\mu_2WZ_2+\ldots$$

$$+k_{r2}(|(u_2-u_1)|-d_2)Sign(u_2-u_1)H<|(u_2-u_1)|-d_2>=-m_2\ddot{u}_g(t) \tag{12}$$

In which Z_2 describes as follow

$$\frac{dZ_2}{dt}=\frac{1}{u_{y2}}\left\{A_2-|Z_2|^{\eta_2}\left[\gamma_2 Sign\left((\dot{u}_2-\dot{u}_1)Z_2\right)+\beta_2\right]\right\}(\dot{u}_2-\dot{u}_1) \tag{13}$$

$$m_1\ddot{u}_1+\frac{W}{R_{eff\,1}}u_1+\mu_1WZ_1+k_{r1}(|u_1|-d_1)Sign(u_1)H<|u_1|-d_2>-\frac{W}{R_{eff\,2}}(u_2-u_1)-\mu_2WZ_2-\ldots$$

$$-k_{r2}(|(u_2-u_1)|-d_2)Sign(u_2-u_1)H<|(u_2-u_1)|-d_2>=-m_1\ddot{u}_g(t) \tag{14}$$

and similarly Z_1 can be obtained as

$$\frac{dZ_1}{dt}=\frac{1}{u_{y1}}\left\{A_1-|Z_1|^{\eta_1}\left[\gamma_1 Sign(\dot{u}_1Z_1)+\beta_1\right]\right\}\dot{u}_1 \tag{15}$$

In the solution procedure, the term including with the second derivative of displacement in (11), (12) and (14) remains on the left-hand side of the equations of motion and the other terms are moved to right-hand side. According to the above equations for seismic isolation system, a program has been written for functions with multi inputs and outputs using Embedded MATLAB Function Block that can be incorporated into a Simulink model. In this model, the blue block in Fig. 4 includes the equation of motion for the mass m_3. The displacement and velocity of the masses m_2 ($u2$ and $u2d$) and m_3 ($u3$ and $u3d$) and the ground acceleration (acclg) are used as the

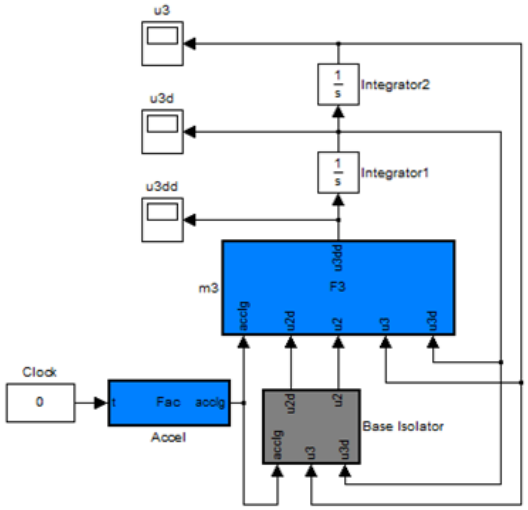

Fig. 4 SIMULINK Model of the schematic model of a one-story base-isolated structure

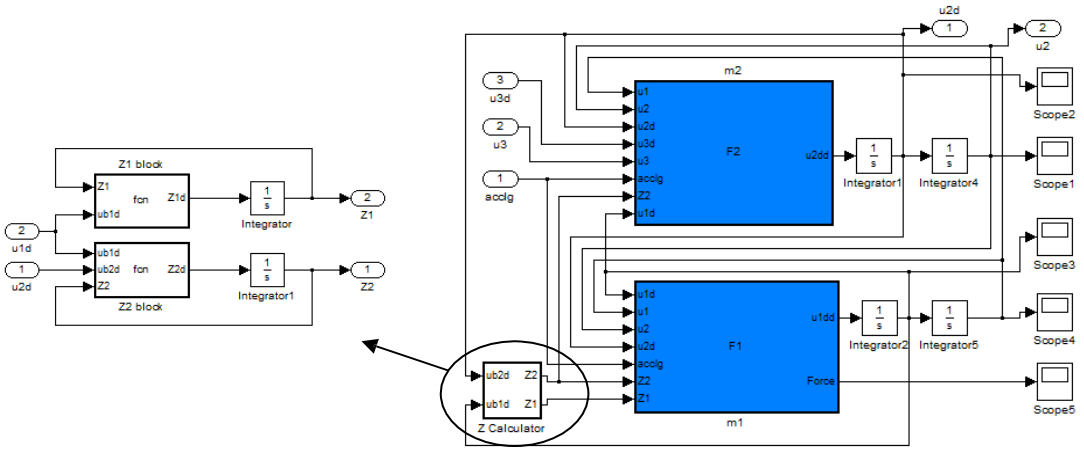

Fig. 5 SIMULINK Model of the isolation system

input in the block related to the mass m_3. The solutions for velocity and displacement of the mass m_3 can be obtained by using SIMULINK integrator, $1/s$. The properties in this state of analysis are used for the solution procedure until state change is detected. In the solution procedure, the final displacement and velocity of one state become the initial conditions for the next state.

On the other hand, the gray block in Fig. 4 includes the equations of motion for the masses of isolation system; m_1 and m_2. As shown in Fig. 5 the input is the displacement and velocity of the mass m_3 ($u3$ and $u3d$) and the ground acceleration (acclg) and the output is the displacement and velocity of the mass m_2 ($u2$ and $u2d$). Moreover, the non-dimensional displacement components Z_1 and Z_2 are computed in this block

Furthermore, the idealized N-story base-isolated building adjacent to fixed-base structure with the same floors considered in the present study. As mentioned before, impact may occur with the adjacent structure either at the base of the isolated building or at the levels of the floors of their superstructures. For instance, a 4-story base-isolated building using the DCFP bearing adjacent to a 4-story fixed-base structure has been modeled and simulated in the MATLAB environment using the Embedded MATLAB Function Block (see Fig. 6). The blue blocks in each floor include the equation of motion for the floor mass and the middle blocks include the impact between two structures. Here, the displacement, velocity and the isolation gap distance between two adjacent structures are used as the input in each block. On one hand, the impact occurrence will be considered if the distance between two masses of the same level in isolated building and the adjacent structure is less than the gap size. On the other hand, the impact will be considered to occur in two phases: the compression phase and the restitution phase based on the relative velocity of two masses. Then, the pounding force is moved to the equations of motion for two masses in each floor.

This SIMULINK toolbox is actually a set of differential equations that contain 12 second-order coupled differential equations (1 differential equation for each floor and 2 differential equations for DCFP bearing) and can be solved by Odesolve MATLAB program. It's well-mentioned that without using SIMULINK toolbox, this set of differential equations should be solved in state space by converting them to the differential equations of first-order that is almost practically impossible according to the large number of equations exist.

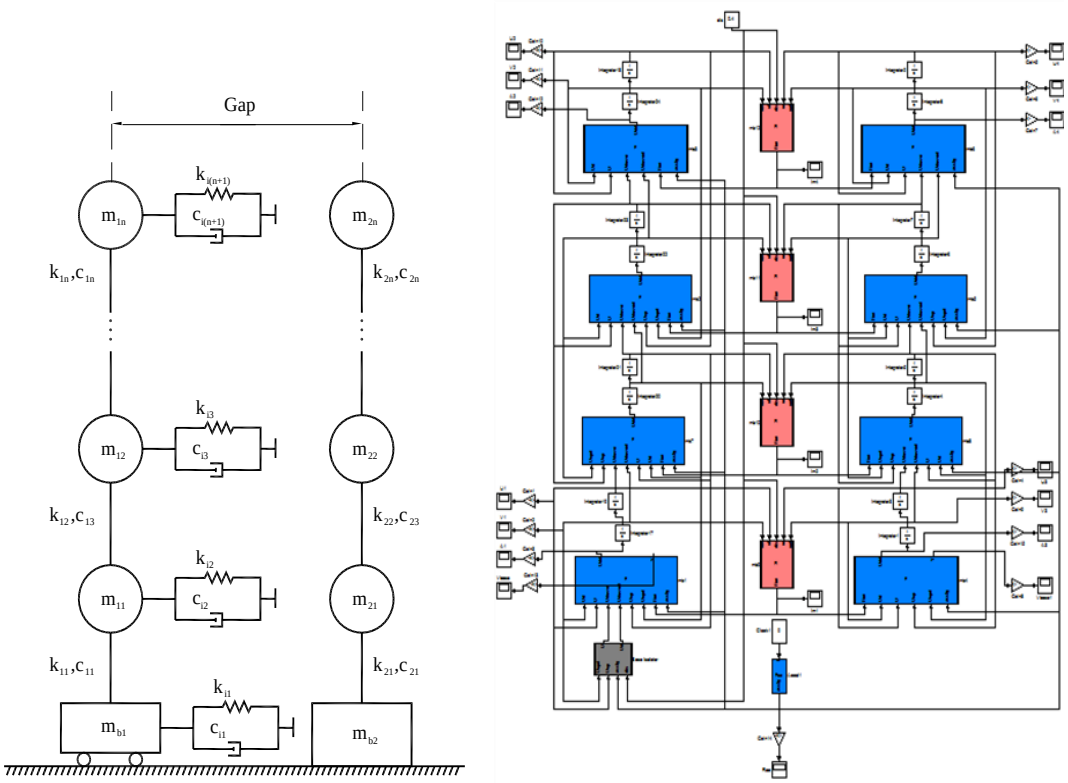

(a) (b)

Fig. 6 (a) Real model and (b) SIMULINK Model of a 4-story isolated building and fixed-base structure when are adjacent to each other

3. Validation of the implemented model

As mentioned before, the DCFP systems consist of two identical sliding surfaces with the same friction coefficients and radius of curvature, which results in friction pendulum systems (FPS) behavior having radius of curvature equal to the summation of radii of curvature of the sliding surfaces in DCFP systems.

In this regard, it is expected that the results related to those DCFPs have enough conformity with results obtained by Almazan *et al*. (1998). This behavior of a DCFP can be achieved by considering the radius of curvature of each sliding surface to be equal to half of the radius of curvature of sliding surface in FPS. Herein, a one-story structure using friction pendulum bearing is investigated. The properties of this model are taken as R=100 cm, μ=0.07 and m_2/m_3=0.2. Fig. 7 shows that the hysteretic behavior of FPS for Newhall ground motion in x-direction has adequate consistency with earthquake response of the structures obtained from models employed by Almazan *et al*. (1998). Notice that the force and displacement in both diagrams have been normalized with respect to the weight of isolated building and radius of curvature of sliding surface respectively.

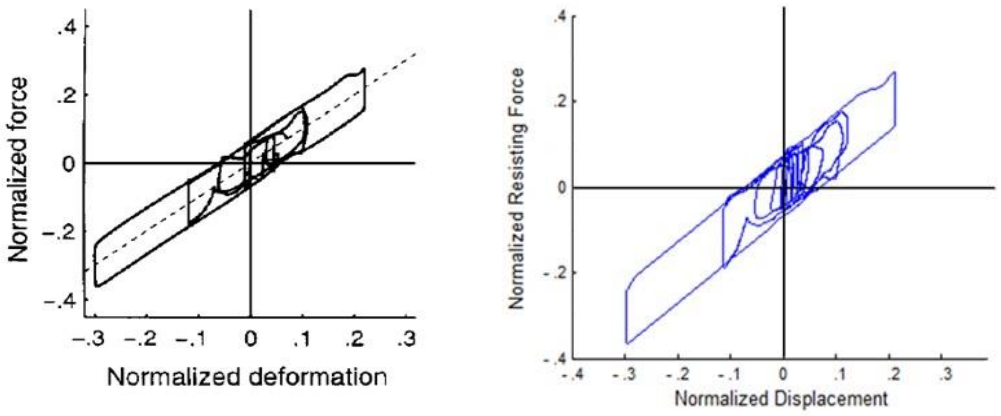

(a) Almazan *et al*. (1998) (b) in the present study

Fig. 7 Comparison between normalized x-direction force-deformation loop for Newhall earthquake

Table 1 Ground motion records specifications

Earthquake	Station	PGA (g)	PGV (cm/sec)
Chi-Chi 1999/09/20	CHY080	0.968	107.5
Erzincan 1992/03/13	95 Erzincan	0.515	83.9
Imperial Valley 1979/10/15	5054 Bonds Corner	0.775	75.3
Kobe 1995/01/16	0 KJMA	0.821	81.3
Northridge 1994/01/17	24279 Newhall - Fire Sta	0.583	75.5
Northridge 1994/01/17	77 Rinaldi Receiving Sta	0.838	166.1
Northridge 1994/01/17	24514 Sylmar - Olive View Med FF	0.843	129.6

Notice that for the numerical study the following parameters are held constant:
a=50 sec/m; u_y=0.1 mm; A=1; β=γ=0.5

4. Parametric study

The effect of impact on seismic performance of base-isolated buildings under various earthquakes induced large deformations is investigated. Nonlinear time history analyses for various earthquake excitations listed in Table 1 are carried out on three isolated structural systems; a 2-story building (T_s=0.25 sec), a 4-story building (T_s=0.5 sec) and an 8-story building (T_s=1.0 sec) to examine the performance of different DCFP isolation systems (T=2, 3, 4 and 5 sec). Therefore, the model of the isolated structural system under consideration can be characterized by specifying the parameters namely, damping ratio of the superstructure which is kept constant for all modes (ξ_s=0.05), number of story in the superstructure (*2-, 4- and 8-story structures*), the period of the isolation system (T) and the fundamental period of superstructure (T_s). For the present study, the mass of each floor is kept constant. Also, for simplicity the stiffness of all stories is taken as constant expressed by the parameter k_s. The value of stiffness is selected somehow to provide the required fundamental period of the superstructure. For all cases, the stiffness, mass and number of stories for base-isolated buildings and adjacent fixed-base structures are the same. Seismic responses such as base shear, displacement in the isolation system and superstructure (top

Table 2 Properties of isolation systems

DCFP	T (sec)	$R1$ (m)	$R2$ (m)
DCFP1	2	0.50	0.50
DCFP2	3	1.12	1.12
DCFP3	4	1.99	1.99
DCFP4	5	3.11	3.11

floor) for different isolation systems during impact upon the adjacent structures are computed to study the behavior of the building during impact and comparative performance of various isolation systems. Also, the effects of variation of system parameters: isolation period, superstructure period, size of seismic gap between two structures and friction coefficient of isolator are contemplated.

4.1 Isolation gap distance between isolated building and adjacent structure

The impact occurs when the absolute bearing displacement exceeds the isolation gap distance between the isolated building and the adjacent structure. Therefore, one of the specific objectives to study is the effects of variation in properties of the adjacent structure such as isolation gap distance on the impact response quantities. Herein, a 4-story isolated building by the DCFP system adjacent to a 4-story fixed-base structure for with and without impact conditions under seven near-field earthquake ground motions is investigated. The normalized responses are plotted against the variation in gap size. The normalization is carried out with responses accordant to no impact condition. The parameters of DCFP system considered are four specific values of isolation period; 2, 3, 4 and 5 sec. with adjacent structure at separation gap distances equal 10, 20, 30 and 40 cm. Furthermore, the fundamental period of non-isolated building and adjacent structure is 0.5 sec. The DCFP systems are characterized by the parameters listed in Table 2 while the friction coefficients are taken as fixed values, $f_{max1}=f_{max2}=0.1$.

Fig. 8 shows the maximum normalized base shear at the base of isolated structure versus the variation in gap distance. The figure clearly indicates that, with impact of isolated structure upon adjacent structure, the base shear increases. This increasing is different due to the different values of isolation period. Lower the value of isolation period, smaller the displacement of structure isolated. This implies the decrease in impact force and consequently the increase in base shear for impact conditions. These results show that due to collision of isolated building upon adjacent structure at a separation gap distance of 40 cm, the normalized base shear increases 10% more than the case of isolated building when there is no impact. The peak value of normalized base shear occurs at the minimum value of seismic gap size i.e., 10 cm, implies that the base shear increases more significantly once the gap between adjacent structures closes. In addition, for higher values of isolation time-period (i.e., 4 and 5 sec.), this increasing will be more intensified. Thus, as it is observed, the increase in normalized base shear for isolation period of 2, 3, 4 and 5 sec. is 58%, 134%, 210% and 264% respectively with respect to no impact condition.

On the other hand, as it is anticipated, the normalized bearing displacement increases during impact. For lower values of isolation period (i.e., 2 sec.), this displacement decreases more under earthquake ground motions. Similar results of peak values of normalized bearing displacement are observed in Fig. 9. The increase in isolator displacement for isolation period of 2, 3, 4 and 5 sec. is 63%, 99%, 104% and 98% respectively.

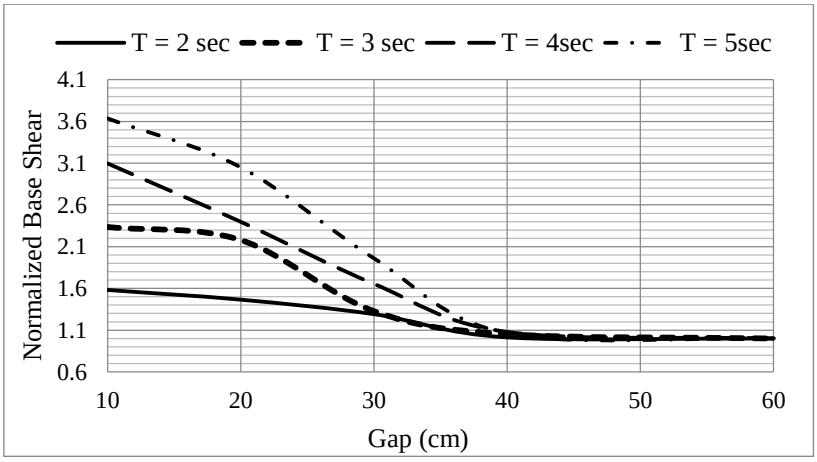

Fig. 8 The maximum normalized base shear on isolated structure vs. the variations of gap distance

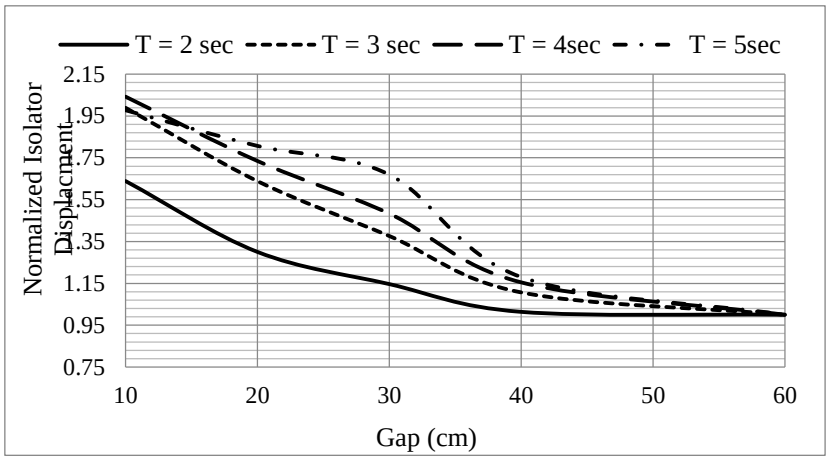

Fig. 9 The maximum normalized isolator displacement vs. the variations of gap distance

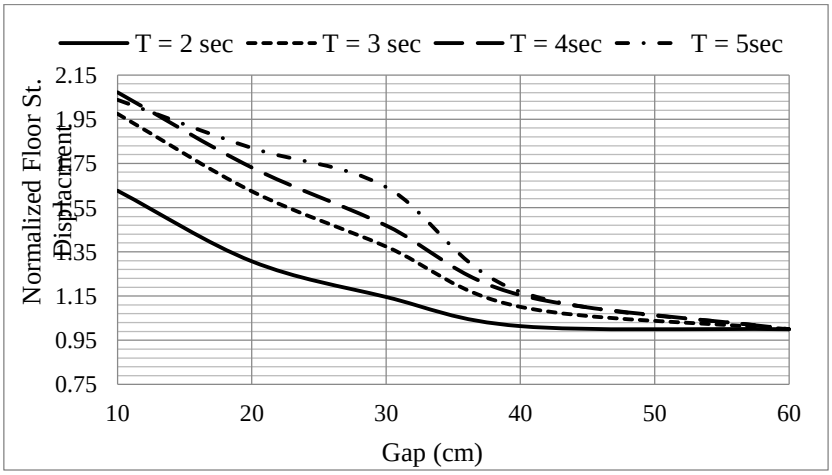

Fig. 10 The maximum normalized top floor (4th story) displacement vs. the variations of gap distance

The plot in Fig. 10 indicates that the normalized displacement in top floor (fourth story) of isolated building has a similar trend to the normalized bearing displacement. Besides, much greater values of impact force would lead to a bearing displacement capacity which would be the greatest. This phenomenon causes the behavior of isolated building tends to a fixed-base structure.

4.2 Friction coefficients of sliding surfaces

The DCFP systems consist of two facing concave surfaces with the same friction coefficient and radius of curvature, which results in bi-linear behavior. The tri-linear behavior of a DCFP can be achieved when the upper and lower concave surfaces have friction coefficients and radii of curvature which are unequal. As mentioned before, unequal coefficients of friction of the two sliding interfaces cause the bearing undergoes sliding on the concave surface having the less coefficient of friction. Then a sufficient horizontal force causes the sliding to initiate on the surface of higher friction coefficient (see Fig. 1).

Effects of variation in friction coefficients of bearings on the dynamic behavior of base-isolated buildings during impact with adjacent structure are studied for a 4-story isolated building in the following sections. The normalized responses are obtained by varying the isolation and superstructure period.

4.2.1 Isolation period

The system is also characterized by bearing isolation period that depends upon radius of curvature of concave surface and friction coefficient. In this section, the specific purpose is to

Table 3 Four isolation system properties (different isolation periods)

	T=2 sec						T=3 sec				
DCFP	$R1$ (m)	$R2$ (m)	f_{max1}	f_{max2}	f_{max2} -f_{max1}	DCFP	$R1$ (m)	$R2$ (m)	f_{max1}	f_{max2}	f_{max2} -f_{max1}
DCFP1	0.5	0.5	0.1	0.1	0	DCFP1	1.12	1.12	0.1	0.1	0
DCFP2	0.5	0.5	0.09	0.11	0.02	DCFP2	1.12	1.12	0.09	0.11	0.02
DCFP3	0.5	0.5	0.08	0.12	0.04	DCFP3	1.12	1.12	0.08	0.12	0.04
DCFP4	0.5	0.5	0.07	0.13	0.06	DCFP4	1.12	1.12	0.07	0.13	0.06
DCFP5	0.5	0.5	0.06	0.14	0.08	DCFP5	1.12	1.12	0.06	0.14	0.08
DCFP6	0.5	0.5	0.05	0.15	0.1	DCFP6	1.12	1.12	0.05	0.15	0.1
DCFP7	0.5	0.5	0.04	0.16	0.12	DCFP7	1.12	1.12	0.04	0.16	0.12
DCFP8	0.5	0.5	0.03	0.17	0.14	DCFP8	1.12	1.12	0.03	0.17	0.14
	T=4 sec						T=5 sec				
DCFP	$R1$ (m)	$R2$ (m)	f_{max1}	f_{max2}	f_{max2} -f_{max1}	DCFP	$R1$ (m)	$R2$ (m)	f_{max1}	f_{max2}	f_{max2} -f_{max1}
DCFP1	0.5	0.5	0.1	0.1	0	DCFP1	1.12	1.12	0.1	0.1	0
DCFP2	0.5	0.5	0.09	0.11	0.02	DCFP2	1.12	1.12	0.09	0.11	0.02
DCFP3	0.5	0.5	0.08	0.12	0.04	DCFP3	1.12	1.12	0.08	0.12	0.04
DCFP4	0.5	0.5	0.07	0.13	0.06	DCFP4	1.12	1.12	0.07	0.13	0.06
DCFP5	0.5	0.5	0.06	0.14	0.08	DCFP5	1.12	1.12	0.06	0.14	0.08
DCFP6	0.5	0.5	0.05	0.15	0.1	DCFP6	1.12	1.12	0.05	0.15	0.1
DCFP7	0.5	0.5	0.04	0.16	0.12	DCFP7	1.12	1.12	0.04	0.16	0.12
DCFP8	0.5	0.5	0.03	0.17	0.14	DCFP8	1.12	1.12	0.03	0.17	0.14

study the effects of variation of friction coefficient of DCFP bearings on the base shear, bearing and top floor displacement. Therefore, a 4-story isolated building adjacent to a 4-story fixed-base structure with a separation gap distance of 20 cm under seven near-field earthquake ground motions is studied. Four DCFPs, i.e. tri-linear and bi-linear DCFPs with the same equivalent frictions ($f_{max,eqv}=f_{max1}=f_{max2}$) but four different isolation periods of 2, 3, 4 and 5 sec. are taken into account (see Table 3). The bearing configuration considered here is equal radii and unequal coefficients of friction. Thus, eight DCFPs are studied for each period of isolation. Herein, similar to last section, the seismic responses taken for understanding the overall behavior of the base-isolated structure with various DCFP isolators are normalized base shear and displacement of isolator and top floor. Figs. 11-13 illustrate that in all cases, the aforementioned seismic responses are normalized with respect to the responses using bi-linear DCFP isolator (equal coefficients of friction). Consequently, they are equal to 1 in the case of $f_{max2}-f_{max1}=0$.

Generally, the isolation systems with higher values of isolation period result in greater values of displacement and smaller values of base shear when there is no impact between isolated and adjacent structures. But, both the base shear and displacements increase more in these isolation systems during impact phenomena. The results indicate that due to increasing in friction coefficient difference ($f_{max2}-f_{max1}$), the normalized displacements are increased which confirms the increasing in impact force and base shear pertaining to impact. The variation of peak normalized base shear is indicated in Fig. 11 with variation in friction coefficient difference for the isolation systems in consideration. The peak value of normalized base shear occurs at the maximum friction coefficient difference. The increase in normalized base shear for isolation period of 2, 3, 4 and 5 sec. is 40%, 28%, 53% and 43% respectively. Also, effects of variation in friction coefficient difference on bearing and top floor displacement are studied for the 4-story isolated building as shown in Figs. 12 and 13 respectively. Similarly, the normalized response of all the systems shows that the maximum increase in the normalized bearing displacement occurs at the maximum friction coefficient difference. The increase in normalized bearing displacement for isolation period of 2, 3, 4 and 5 sec. is 27%, 25%, 29% and 25% respectively. Similar trend of increase in the normalized top floor displacement is observed. This implies that the behavior of isolated building tends to a fixed-base structure and the displacements occur at the isolation level.

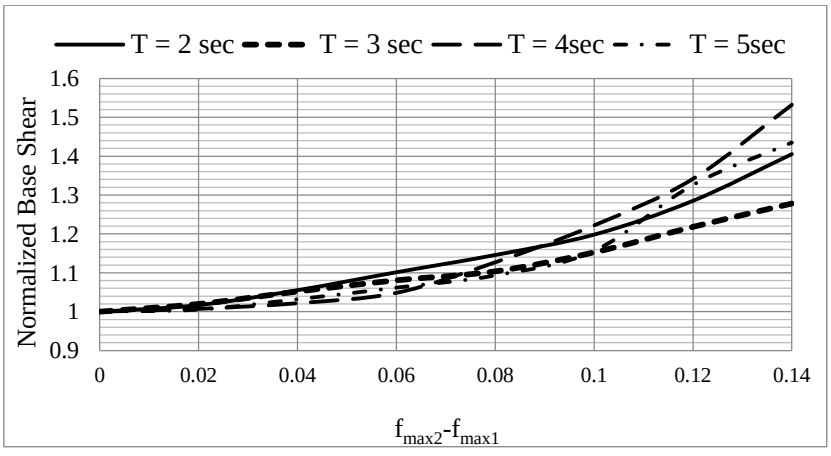

Fig. 11 The maximum normalized base shear vs. the variations of friction coefficient difference considering various isolation periods (T)

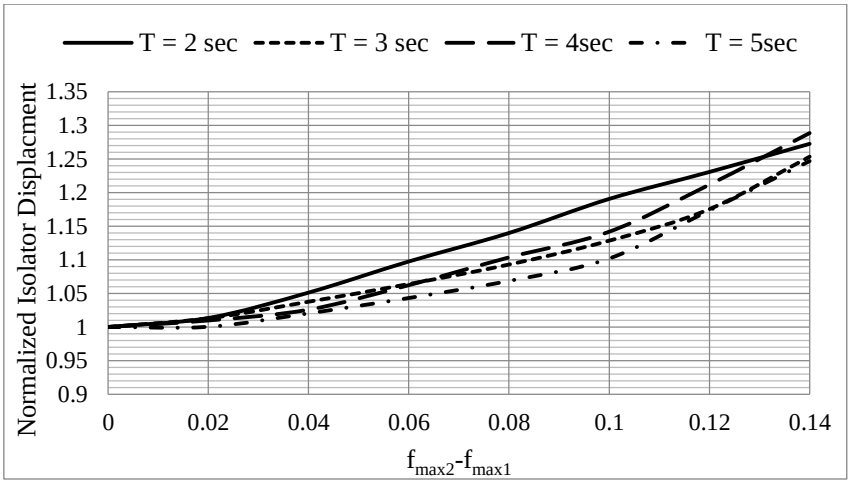

Fig. 12 The maximum normalized bearing displacement vs. the variations of friction coefficient difference considering various isolation periods (T)

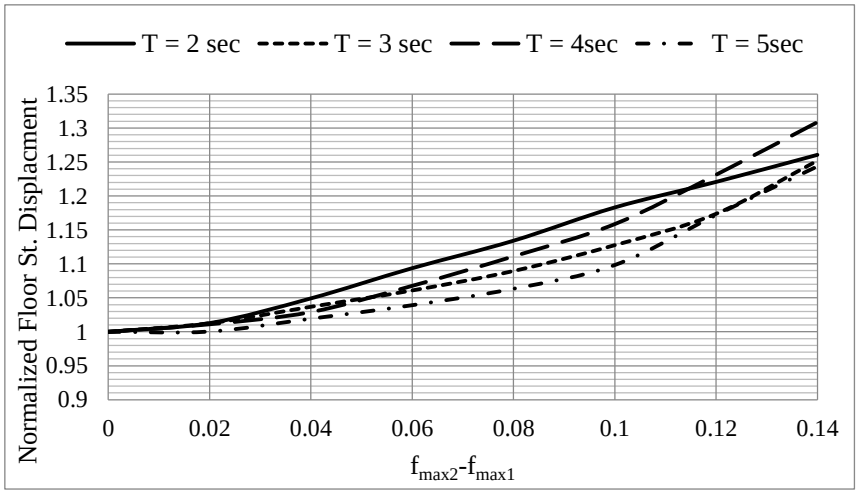

Fig. 13 The maximum normalized top floor (4th story) displacement vs. the variations of friction coefficient difference considering various isolation periods (T)

4.2.2 Period of superstructure

In order to study the effects of flexibility of superstructure, the peak normalized base shear, bearing and top floor displacement are obtained for the isolated building with impact condition under seven near-field earthquakes as shown in Figs. 14-16 respectively. With varying in number of story and period of superstructure, three isolated structural systems; a 2-story building (T_s=0.25 sec), a 4-story building (T_s=0.5 sec) and an 8-story building (T_s=1.0 sec) are investigated. Additionally, it's well-mentioned that the adjacent structures considered have the same properties of number of story and natural period of vibration as the isolated structural systems. The isolation systems considered are listed in Table 3 (Isolation system with isolation period of 4 sec.) with isolation gap distance is equal to 20 cm.

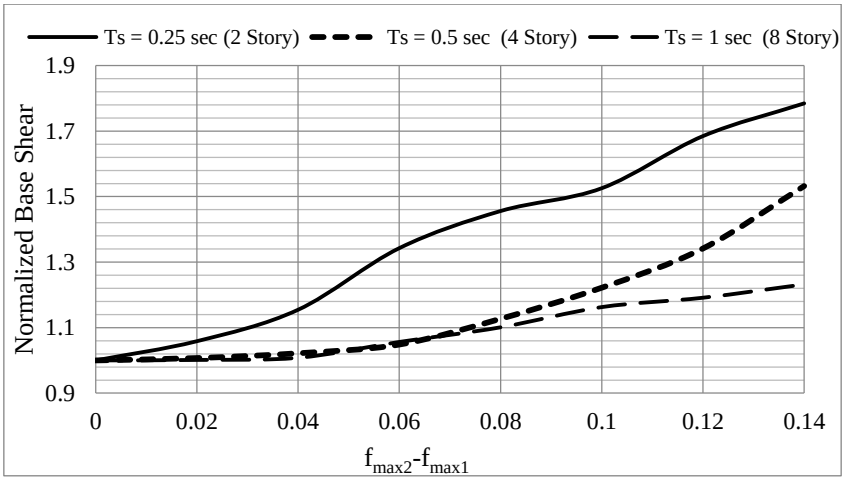

Fig. 14 The maximum normalized base shear vs. the variations of friction coefficient difference considering various superstructure periods (T_s)

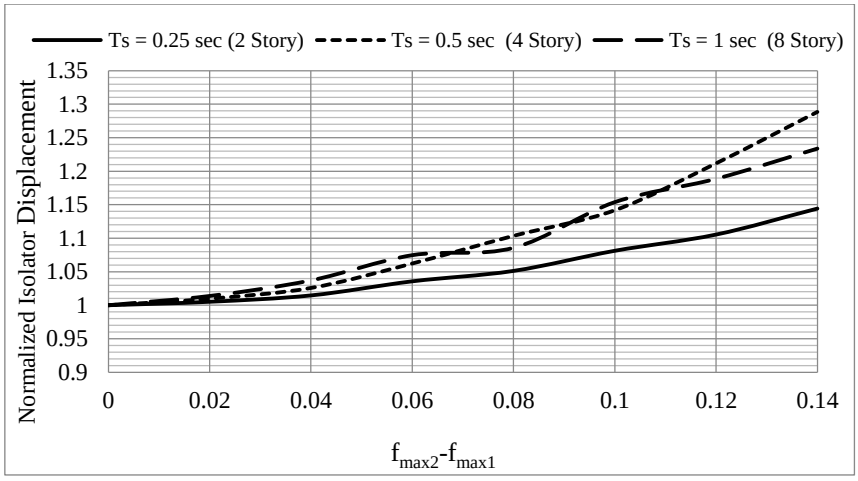

Fig. 15 The maximum normalized isolator displacement vs. the variations of friction coefficient difference considering various superstructure periods (T_s)

It is seen from Fig. 14 that the superstructures normalized base shear goes on increasing with the increase in friction coefficient difference. The normalized base shear increases significantly during earthquakes in the superstructures having lower period. The peak values of normalized base shear occurs at the maximum values of friction coefficient difference. These peak values for 2-, 4- and 8-story buildings are 78%, 53% and 23% respectively more than the case of bi-linear DCFP which have identical friction coefficients (μ_1=μ_2). In addition, the normalized bearing and top floor displacement show a trend of increase with the increase in friction coefficient difference (Figs. 15 and 16). The variation of peak normalized bearing displacement with variation in number of story shows that the maximum values of increase in displacement for the 2-, 4- and 8-story isolated buildings in consideration are 14%, 28% and 23% respectively more than the case of equal friction coefficients.

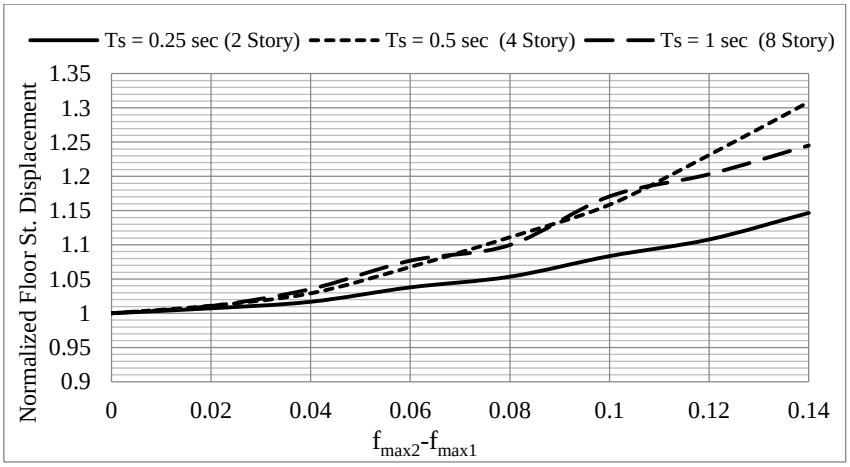

Fig. 16 The maximum normalized top floor displacement vs. the variations of friction coefficient difference considering various superstructure periods (T_s)

5. Conclusions

Numerical investigations are carried out on the response of multi-story seismically isolated building supported on various base isolation systems during impact with adjacent structures. In this study, a brief review on the commonly used impact analytical models is conducted. Based on this review, a non-linear viscoelastic impact model of pounding force which is intended to enhance the accuracy of the modeling of structural pounding during near-field earthquakes is implemented. Nonlinear time history analyses are carried out on three isolated structural systems; a 2-story building (T_s=0.25 sec), a 4-story building (T_s=0.5 sec) and an 8-story building (T_s=1.0 sec) to examine the performance of different DCFP isolation systems (i=2, 3, 4 and 5 sec) under seven earthquake inputs. Parametric studies are conducted on base-isolated structure to observe the influence of different parameters such as period of isolation system and superstructure, gap distance, radius of curvature of the sliding surface and friction coefficient of isolator on the impact response.

The results of this study are summarized as follows:

• The normalized base shear, bearing and top floor displacement increase significantly due to the impact upon the adjacent structure during an earthquake. As the gap distance between base-isolated building and the adjacent structure decreases, there is increase in impact force and consequently in base shear. This increasing is different due to the different values of isolation period, i.e. the normalized base shear is increased significantly with increased isolation period. The peak value of normalized base shear occurs at the minimum value of seismic gap size and maximum value of isolation period i.e., 10 cm and 5 sec. respectively (264% more than the case of isolated building when there is no impact). Normalized bearing and top floor displacement increase with reduction in gap distance (104% more than the case of isolated building when there is no impact).

• With increase in friction coefficients of the sliding surfaces, there is marginal increase in normalized base shear, bearing and top floor displacement due to the period of isolation. Both the base shear and displacements increase more in isolation systems with higher values of

isolation period during impact phenomena. However, variation in number of story and consequently fundamental period of superstructure has significant effect on response quantities. The lower superstructure (2-story building) during impact phenomenon **is**, in general, found more affected than the 4- and 8-story structures considering the variation in friction coefficient difference. The peak value of normalized base shear is 78% more than the case of bi-linear DCFP which have identical friction coefficients.

• Increased flexibility of superstructure decreases the increasing in normalized base shear during impact as compared to that in case of bi-linear DCFP which have identical friction coefficients. Also, the normalized bearing displacement is increased marginally (at most 28% more than the case of equal friction coefficients) with increased flexibility.

Rerences

Agarwal, V.K., Neidzweeki, J.M. and Van de lindt, J.W. (2007), "Earthquake induced pounding in friction varying base isolated buildings", *Eng. Struct.*, **29**(11), 2825-32.

Almazan, J.L., De la llera, J.C. and Inaudi, J.A. (1998), "Modeling aspects of structures isolated with the frictional pendulum system", *Earthq. Eng. Struct. Dyn.*, **27**(8), 845-867.

Anagnostopoulos, S.A. (1988), "Pounding of buildings in series during earthquakes", *Earthq. Eng. Struct. Dyn.*, **16**, 443-456.

Constantinou, M.C. (2004), Friction Pendulum Double Concave Bearing, Available at: http://nees.buffalo.edu/dec304/FP-DC%20Report-DEMO.pdf.

DesRoches, R. and Muthukumar, S. (2002), "Effect of pounding and restrainers on seismic response of multiple-frame bridges", *J. Struct. Eng.*, ASCE, **128**, 860-869.

Fenz, D.M. and Constantinou, M.C. (2006), "Behavior of the double concave friction pendulum bearing", *Earthq. Eng. Struct. Dyn.*, **35**(11), 1403-1424.

Fenz, D.M. (2008), "Behavior of the double concave friction pendulum bearing", Ph.D. Dissertation, The State University of New York at Buffalo, NY.

Filiatrault, A., Wagner, P. and Cherry, S. (1995), "Analytical prediction of experimental building pounding", *Earthq. Eng. Struct. Dyn.*, **24**, 1131-1154.

Goldsmith, W. (1960), *Impact: The Theory and Physical Behavior of Colliding Solids*, Edward Arnold, London.

Hyakuda, T., Saito, K., Matsushita, T., Tanaka, N., Yoneki, S., Yasuda, M., Miyazaki, M., Suzuki, A. and Sawada, T. (2001), "The structural design and earthquake observation of a seismic isolation bearing using friction pendulum system", *Proceedings of the 7th International Seminar on Seismic Isolation, Passive Energy Dissipation and Active Control of Vibration of Structure*, Assisi, Italy, October.

Jankowski, R. (2005), "Non-linear viscoelastic modeling of earthquake-induced structural pounding", *Earthq. Eng. Struct. Dyn.*, **34**, 595-611.

Jankowski, R. (2006), "Analytical expression between the impact damping ratio and the coefficient of restitution in the non-linear viscoelastic model of structural dynamic", *Earthq. Eng. Struct. Dyn.*, **35**, 517-527.

Kelly, J.M. (1986), "A seismic base isolation: review and bibliography", *Soil Dyn. Earthq. Eng.*, **5**(3), 202-216.

Khoshnoudian, F. and Haghdoust, V. (2009), "Response of pure-friction sliding structures to three components of earthquake excitation considering variation in the coefficient of friction", *Scientia Iranica, Tran. A. Civil Eng.*, **16**(6), 1-16.

Khoshnoudian, F. and Rabiei, M. (2010), "Seismic response of double concave friction pendulum base-isolated structures considering vertical component of earthquake", *Adv. Struct. Eng.*, **13**(1), 1-14.

Kim, S.H. and Shinozuka, M. (2003), "Effects of seismically induced pounding at expansion joints of

concrete bridges", *J. Eng. Mech.*, ASCE, **129**, 1225-1234.
Kim, Y.S. and Yun, C.B. (2007), "Seismic response characteristics of bridges using double concave friction pendulum bearings with tri-linear behavior", *Eng. Struct.*, **29**(11), 3082-3093.
Komodromos, P., Polycarpou, P.C., Papaloizou, L. and Phocas, M.C. (2007), "Response of seismically isolated buildings considering poundings", *Earthq. Eng. Struct. Dyn.*, 36, 1605-1622.
Komodromos, P. (2008), "Simulation of the earthquake-induced pounding of seismically isolated buildings", *Comput. Struct.*, **86**, 618-626.
Maison, B.F. and Kasai, K. (1992), "Dynamics of pounding when two buildings collide", *Earthquake Earthq. Eng. Struct. Dyn.*, 21, 771- 786.
Malhotra, P.K. (1997), "Dynamics of seismic impacts in base-isolated buildings", *Earthq. Eng. Struct. Dyn.*, **26**, 797-813.
Matsagar, V.A. and Jangid, R.S. (2003), "Seismic response of base-isolated structures during impact with adjacent structures", *Eng. Struct.*, 25, 1311-1323.
Mostaghel, N. and Khodaverdian, M. (1987), "Dynamics of resilient-friction base isolator (R- FBI)", *Earthq. Eng. Struct. Dyn.*, **15**(3), 379-390.
Mostaghel, N. and Tanbakuchi, J. (1983), "Response of sliding structures to earthquake support motion", *Earthq. Eng. Struct. Dyn.*, **11**(6), 729-748.
Mokha, A., Constantinou, M.C., Reinhorn, A.M. and Zayas, V. (1991), "Experimental study of friction pendulum isolation system", *Struct. Eng.*, ASCE, **117**(4), 1201-1217.
Murnal, P. and Sinha, R. (2002), "Earthquake resistant design of structures using the variable frequency pendulum isolator", *Struct. Eng.*, ASCE, **128**(7), 870-880.
Muthukumar, S. and DesRoches, R.A. (2006), "Hertz contact model with nonlinear damping for pounding simulation", *Earthq. Eng. Struct. Dyn.*, **35**(7), 811-828.
Nagarajaiah, S. and Sun, X. (2001), "Base-isolated FCC building: impact response in Northridge earthquake", *Struct. Eng.*, ASCE, **127**(9), 1063-1075.
Panayiotis, P.C. and Komodromos, P. (2010), "Earthquake-induced poundings of a seismically isolated building with adjacent structures", *Eng. Struct.*, **32**, 1937-1951.
Panchal, V.R. and Jangid, R.S. (2008), "Seismic behavior of variable frequency pendulum isolator", *Earthq. Eng. Eng. Vib.*, **7**(2), 193-205.
Ruangrassamee, A. and Kawashima, K. (2001), "Relative displacement response spectra with pounding effect", *Earthq. Eng. Struct. Dyn.*, **30**, 1511-1538.
Skinner, R.I., Robinson, W.H. and McVerry, G.H. (1993), *An Introduction to Seismic Isolation*, Wiley, Chichester.
Su, L., Ahmadi, G. and Tadjbakhsh, I.G. (1989), "A comparative study of performance of various base isolation systems, Part I: shear beam structures", *Earthq. Eng. Struct. Dyn.*, **18**(1), 11-32.
Tsai, H.C. (1997), "Dynamic analysis of base-isolated shear beams bumping against stops", *Earthq. Eng. Struct. Dyn.*, **26**, 515-528.
Tsai, C.S., Chiang, T.C. and Chen, B.J. (2003), "Seismic behavior of MFPS isolated structure under near-fault sources and strong ground motions with long predominant periods", *ASME Pressure Vessels and Piping Conference, Seismic Engineering*, Ed. Chen, J.C., Cleveland, Ohio, USA.
Tsai, C.S., Chen, B.J., Pong, W.S. and Chiang, T.C. (2004), "Interactive behavior of structures with multiple friction pendulum isolation system and unbounded foundations", *Adv. Struct. Eng.*, **7**(6), 539-551.
Tsai, C.S., Chiang, T.C. and Chen, B.J. (2005), "Experimental evaluation of piecewise exact solution for predicting seismic responses of spherical sliding type isolated structures", *Earthq. Eng. Struct. Dyn.*, **34**(9), 1027-1046.
Tsopelas, P., Constantinou, M.C., Kim, Y.S. and Okamoto, S. (1996), "Experimental study of FPS system in bridge seismic isolation", *Earthq. Eng. Struct. Dyn.*, **25**(1), 65-78.
Yang, Y.B., Lee, T.Y. and Tsai, I.C. (1990), "Response of multi-degree-of-freedom structures with sliding supports", *Earthq. Eng. Struct. Dyn.*, **19**(5), 739-752.

Ye, K. and Li, L. (2009), "Impact analytical models for earthquake-induced pounding simulation", *Fron. Arch. Civil Eng. China*, **3**, 142-147.

Zanardo, G., Hao, H. and Modena, C. (2002), "Seismic response of multi-span simply supported bridges to a spatially varying earthquake ground motion", *Earthq. Eng. Struct. Dyn.*, **31**, 1325-1345.

Zayas, V.A., Low, S.S. and Mahin, S.A. (1990), "A simple pendulum technique for achieving seismic isolation", *Earthq. Spectra*, **6**(2), 317-333.